

RESEARCH PAPER

Green Synthesis and Morphology Dependent Antibacterial Activity of Copper Oxide Nanoparticles

Shima Tavakoli¹, Mahshid Kharaziha^{1*}, Shokouh Ahmadi²

¹ Department of Materials Engineering, Isfahan University of Technology, Isfahan, Iran

² Department of Food Science and Technology, College of Agriculture, Isfahan University of Technology, Isfahan, Iran

ARTICLE INFO

Article History:

Received 09 October 2018

Accepted 24 December 2018

Published 01 January 2018

Keywords:

Aloe Vera

Antibacterial property

Copper oxide nanoparticle

Green synthesise

ABSTRACT

Copper oxide nanoparticle (CuO-NPs) has been widely utilized in biomedical application due to their antibacterial function. It is well known that antibacterial characteristics of materials could be controlled using the size, shape and composition of the particles. The aim of this paper is to green synthesis CuO-NPs with various morphologies, using Aloe Vera extract as reducing agent and investigate the effect of particle size and shape on the antibacterial properties. Results demonstrated the formation of pure CuO-NPs with crystallite size in range of 9-23 nm, depending on the precursor type and concentration as well as aging time. Furthermore, increasing the concentration of copper precursor from 6 mM to 1M altered the morphology from rod shape to spherical. We also examined the inhibitory effects of CuO-NPs toward the gram-negative bacterium, Escherichia coli and a gram-positive bacterium, Staphylococcus aureus cultures throughout a 24 hr period. Based on our data, while CuO-NPs had significant growth inhibition, this property depended on the morphology and size of particles. Rod shape CuO-NPs with smooth surface were the most effective morphology due to the largest surface area contacting and highest reactivity in contact with bacteria. Results also demonstrated that St aureus was more resistant to CuO-NPs samples because it was a Gram positive bacteria and Gram-negative ones like E. coli were more susceptible, while all particles were toxic to both organisms. Together, these results suggest that the difference between the surface free energy may be a cause for their morphology-dependent antimicrobial activity.

How to cite this article

Tavakoli S, Kharaziha M, Ahmadi S. Green Synthesis and Morphology Dependent Antibacterial Activity of Copper Oxide Nanoparticles. J Nanostruct, 2019; 9(1):163-171. DOI: 10.22052/JNS.2019.01.018

INTRODUCTION

In the recent years, metal nanoparticles have been widely applied in various fields consisting of electrical, magnetic, catalytic and biological activities due to their unique physical and chemical characteristics [1-3]. In particular, copper oxide nanoparticles (CuO-NPs) have been broadly studied in various fields including agriculture, fabrics, and especially in hospital and clinical applications due to their unique biological and antibacterial properties, with high efficiency for

* Corresponding Author Email: ma.kharaziha@gmail.com

a broad spectrum of microorganisms, and fewer prices compared to noble metals with similar properties [4-6].

CuO-NPs can be synthesized using various approaches consisting of hydrothermal [7], solution combustion [8], precipitation [9], electrochemical [10], microwave assisted [11], chemical [12], force hydrolysis [13], sol-gel [14], reverse microemulsion [15] and sono-chemical [16] techniques. Most of these approaches are eco-hazardous limiting their applications in medicine and bioengineering.

Therefore, attentions have focused to develop eco-friendly techniques such as biosynthesis method by employing microorganisms such as bacterial and fungi, as well as whole plants, tissues and extracts [17]. Recently, the extracts of plants such as Geranium leaf, Catharanthus roseus and lemongrass have been applied to stabilize and reduce the metal ions such as ZnO [18], In_2O_3 [19], Fe_xO_y [20], gold (Au) and silver (Ag) [21] nanoparticles. Between various kinds of the plant, Aloe vera plant has been widely applied to green synthesize various kinds of metal and metal oxides [22, 23]. Aloe vera comprises of about 75 potentially active constituents, which possess immunomodulatory, anti-inflammatory, antiparasitic and wound or burn-healing characteristics [24]. Aloe vera extracts have recently applied in order to synthesize copper based nanomaterials such as CuO, Cu and etc. For instance, Kumar et al. [25] synthesized spherical like CuO nanoparticle with average crystallite size of 22 nm using Aloe vera extracts and evaluated their antibacterial characteristics against three bacterial fish pathogens.

Researches demonstrated that nanoparticles with various sizes, morphologies, chemical compositions and surface charges have different antibacterial characteristics which could be due to different ability to generation reactive oxygen species (ROS) and their corresponding ions from nanoparticles [26-29]. Results demonstrated that the antibacterial characteristics of nanoparticles often stems from the production of ROS from nanoparticles which result in oxidative damages to cell construct [30]. For instance, Azam et al. [31] revealed the particle size-dependent antibacterial characteristics of chemically synthesized CuO nanoparticles against gram-positive and negative bacterial strains. In another study, Xiong et al. [26] studied the effects of various morphologies of Cu/Cu₂O nanoparticles consisting of polyhedral, flower-like, and thumbtack-like on the antibacterial activities. They used chemical reducing agent to synthesize Cu/Cu₂O nanoparticles. Peng et al. [27] applied glycine-mediated mixed-solvothermal approach to synthesize Cu₂O with various morphologies from cubic to octahedral. They revealed that the antibacterial properties changed from general bacteriostasis to high selectivity by changing the morphology of nanoparticles from cubic to octahedral.

This work is aimed to find out for the first

time how the biosynthesis parameters affect on the size and morphology of CuO nanoparticles. Furthermore, the effects of these morphology changes on the antibacterial activities against various bacterial organisms are studied. In this study, we adopted a green chemistry approach for the synthesis of CuO-NPs with various morphologies and sizes using the extract plant of Aloe Vera as reducing agent and investigated the effects of biosynthesis parameters on the antibacterial activities against various bacterial organisms. Furthermore, the antibacterial properties of CuO-NPs were studied against a Gram negative, Escherichia coli (E. coli) and a gram-positive, Staphylococcus aureus (St. aureus) bacteria. Results of this study may provide a new strategy to gain effective antibacterial activities via at least price and eco-friendly approach.

MATERIALS AND METHODS

Materials

Copper (II) chloride salt ($\text{CuCl}_2 \cdot 2\text{H}_2\text{O}$), Copper (II) sulfate ($\text{CuSO}_4 \cdot 5\text{H}_2\text{O}$) and sodium hydroxide (NaOH) were purchased from Merck Co. and used as received without further purification. Double distilled (DI) water was used in all the sections of experiment.

Preparation of Aloe Vera leaf extract

Fresh leaves of two-year Aloe Vera were washed with DI water and then dried, completely. Washed, dried and cut leaves (25 g) were added to DI water (30 ml) and kept for 30 min at 110°C in oven until the color of aqueous solution changed from watery to light yellow. After that, the mixture was stirred for 30 min at 110 °C. As prepared solution was passed through a whatman filter paper to remove any solid particle. Finally, the solution was stored at 4 °C as stock for the synthesis of copper oxide (CuO).

Synthesis of copper oxide nanoparticles (CuO-NPs)

In order to synthesize CuO-NPs with various morphologies, two copper precursors were applied: $\text{CuCl}_2 \cdot 2\text{H}_2\text{O}$ and $\text{CuSO}_4 \cdot 5\text{H}_2\text{O}$. The biosynthesis process is depicted in Fig. 1. Aloe Vera extract was added to the aqueous solutions of copper precursor, stirred at 110 °C for 30 min and then kept at 100 °C for 45 min in oven. As prepared solutions were maintained for 72 hr (aging time) to change their color to yellow for samples C and D, and green for samples A, B and

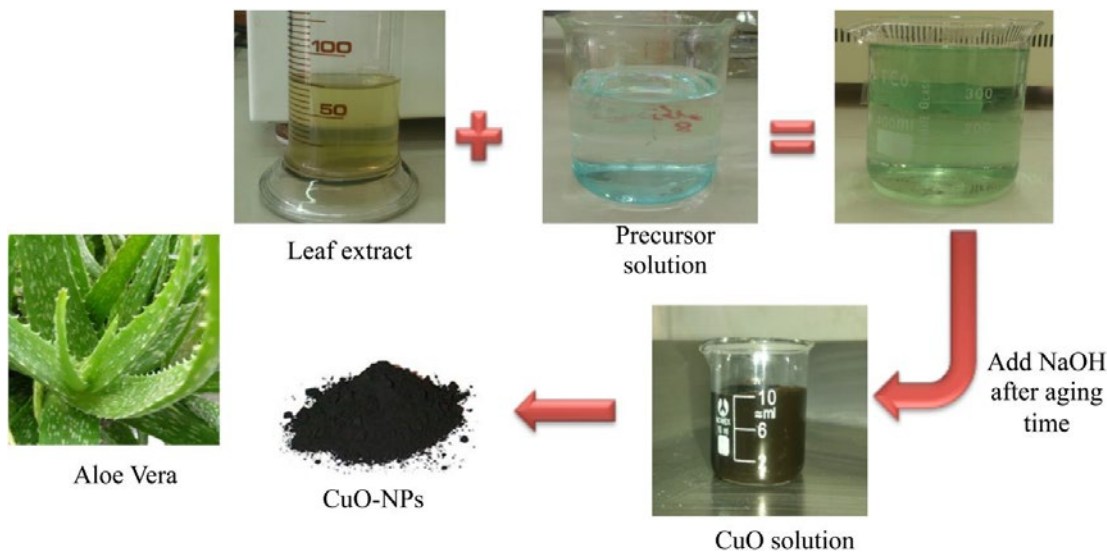


Fig. 1. Schematic representing the synthesis of CuO-NPs by using Aloe Vera extracts as reducing agents

E. Afterwards, the aqueous solution of NaOH was added drop by drop to change the color of as-prepared solutions to brown. In order to prepare CuO-NPs with various morphologies and size, the concentration of solution and aging time were changed (as in Table 1). Finally, after centrifuging for 10 min, as-precipitated CuO-NPs were taken out for characterization.

Characterization of copper oxide nanoparticles (CuO-NPs)

Phase structure analysis of CuO-NPs was carried out by X-ray diffractometer (XRD, Philips X-pert) using Ni filtered Cu Kα (λ CuKα=0.154186 nm, radiation at 40 kV and 30 mA) over the 2θ range of 30–80° (time per step: 2.5 sec and step size: 0.05°). The average crystallite size was estimated using broadening XRD peaks and Scherrer equation (Eq. (1)):

$$t = \frac{k\lambda}{\beta \cos\theta} \tag{1}$$

where λ is the wavelength (0.15406 nm), θ is the Bragg angle, k is a constant (0.9), and t is the crystallite size (nm). For this purpose, three diffraction peaks of (111) and (200), which have the advantages of being well-separated and high intensities, were chosen for the determination of crystallite size. Sigma plot software was also applied to calculate the half-widths of peaks.

The morphology of the powders was investigated by scanning electron microscopy (SEM Phillips XL 30: Eindhoven, The Netherlands). Before imaging, the powders were sputter-coated with a thin layer of gold and the SEM images were utilized to determine the average particle sizes (n=20) using (NIH) Image J software.

Table1. The concentration of copper precursors, NaOH and Aloe Vera as well as aging time in 100 ml aqueous solutions.

Sample	Aloe Vera (ml)	Precursors/ Concentration (M)	NaOH (M)	Aging time (hr)*
A	15	CuCl ₂ .2H ₂ O/1M	15	72
B	15	CuCl ₂ .2H ₂ O /1M	15	0
C	15	CuCl ₂ .2H ₂ O/6mM	15	72
D	15	CuCl ₂ .2H ₂ O/6mM	1	72
E	15	CuSO ₄ .5H ₂ O/1M	15	72

*: Time for maintaining the solution before adding NaOH.



Antibacterial activity of copper oxide nanoparticles (CuO-NPs)

The antibacterial activity of CuO-NPs was studied against a Gram negative bacteria (*E. coli*) and a gram-positive bacterium (*St. aureus*) using well-diffusion agar assay. Bacterial strains were obtained from Persian Type Culture Collection (PTCC) and maintained on Mueller Hinton (MH) slants. A loopful of slant culture was inoculated into Tryptic Soy Broth (Merck, Germany) and incubated at 37 °C for 18 hr (Memert, Germany) until the population of bacteria reached 10^8 CFU/mL. 100 μ L of broth culture were poured into sterile petri dishes and then 25 mL of molten Mueller Hinton Agar Media (Merck, Germany) (45 °C) was added to each petri dish and the plates were gently agitated until the bacteria were spread through whole culture media. The wells were made using the bottom of sterile pasture pipets and the special concentration of nanoparticles suspension containing 10 μ g of CuO-NPs was loaded into the wells. The plates were incubated at 37 °C for 24 hr. Finally, the zone of growth inhibition was measured as antibacterial activity of samples. Three replicates were maintained for each sample and the data presented as mean \pm SD (standard error of the mean).

Statistical analysis

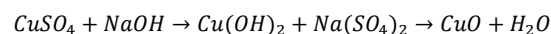
GraphPad, Prism Software (V.5) was used to determine statistical significance in particle and crystallite size results using one-way ANOVA analysis followed by Tukey's multiple comparison. $P \leq 0.05$ was considered statistically significant.

Furthermore, analysis of variance in antibacterial activity evaluation was performed by SAS™ 9.2 software (SAS institute, USA) to compare mean values using LSD test at $P \leq 0.05$ significance level.

RESULTS AND DISCUSSION

Characterization of CuO-NPs

XRD patterns demonstrated while pure CuO-NPs were synthesized in samples A, B and E, the secondary phase of $\text{Cu}(\text{OH})_2$ could be detected in samples C and D (Fig. 2(a)). However, the major peaks of CuO located at $2\theta = 35.70^\circ$ and 38.65° (indexed as (110) and (111) planes based on JCPDS no. 05-0667) could be detected in the samples C and D confirming incomplete formation process of CuO based on following equations:



Based on these equations, $\text{Cu}(\text{OH})_2$ synthesized during the process, could act as nuclei for the growth of CuO-NPs. Therefore, when Cu^{2+} and OH^- concentrations reached the crucial value, CuO nuclei formed spontaneously in the aqueous solution. Based on our data, the low concentrations of CuCl_2 (6 mM) and NaOH (1 M) were not enough to complete the equations 2 and 3 leading to the formation of $\text{Cu}(\text{OH})_2$ as the secondary phase in samples C and D.

The average crystallite size of CuO-NPs was estimated in the range of 9-23 nm, depending on the precursor conditions (Fig. 2(b)). Samples C and

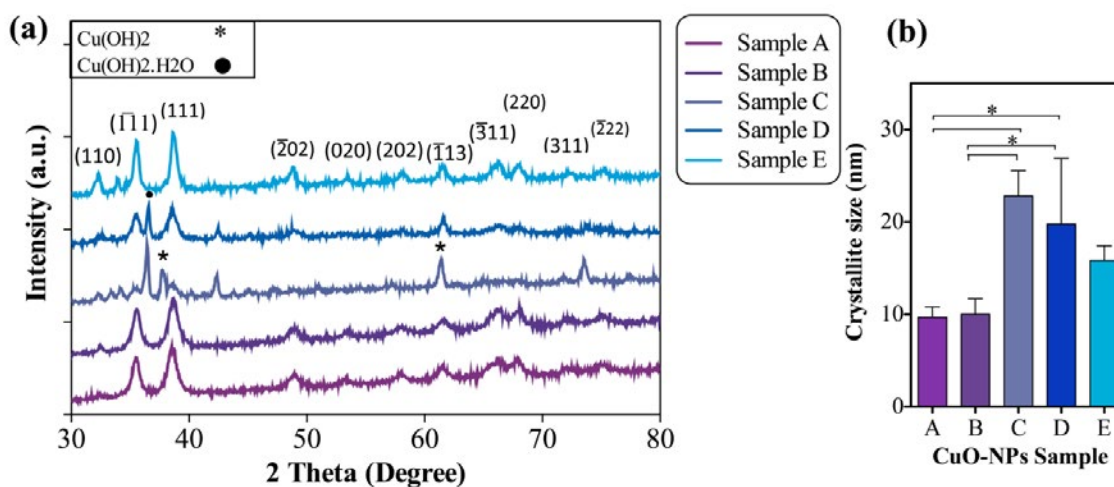


Fig. 2. XRD pattern of CuO-NPs synthesized in various conditions using Aloe Vera leaves extract.

D revealed significantly bigger crystallite size than samples A and B ($P < 0.05$) demonstrating the crucial role of NaOH concentration on the controlling the crystallization of CuO-NPs. When NaOH to CuCl_2 concentration ratio increased (sample C compared to B), the crystallite size of the CuO-NPs enhanced. Based on these results, through choosing the appropriate $\text{Cu}^{2+}/\text{OH}^-$ concentration ratio, the crystallite growth of CuO-NPs could be controlled.

Similar result was reported in previous report [32].

SEM micrograph of the synthesized CuO-NPs demonstrated the effective roles of precursor concentration and type as well as aging time on the morphology and size of CuO-NPs (Fig. 3 (a-e)). While the morphology of particles synthesized via A, D and E conditions were spherical, samples B and C consisted of platelet particles with sharp edges and rod shape, respectively. Additionally,

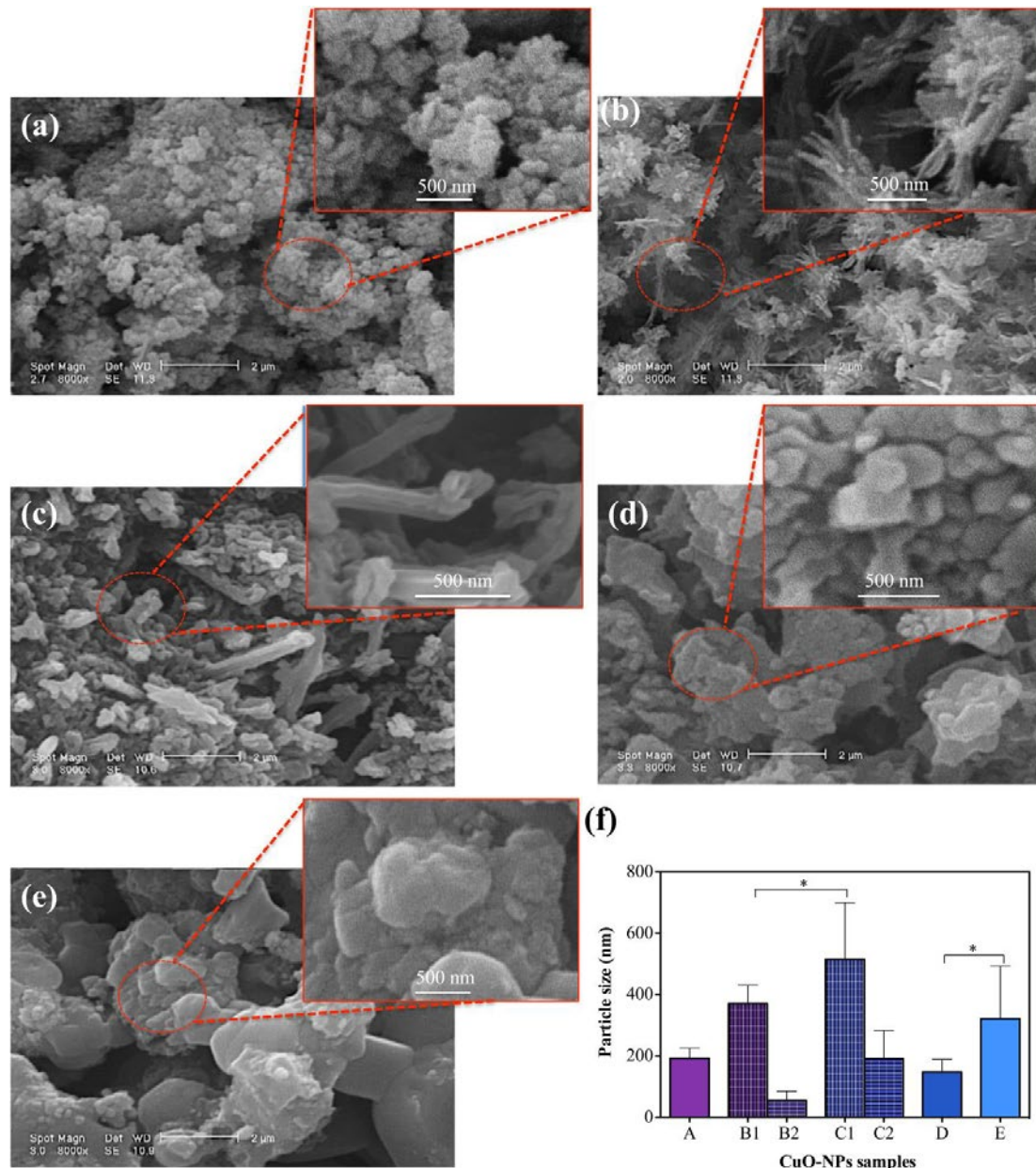


Fig. 3. SEM micrograph of sample (a) A, (b) B, (c) C, (d) D, (e) E as well as (f) the average particles size of CuO-NPs synthesized using Aloe Vera. The particle size of samples B and C was determined in two directions due to the rod-shape morphology: B1 and C1 were length and B2 and C2 were width (* $P < 0.05$).

sample E consisted of spherical plate-particles with smooth surface. The average particle sizes determined using image J software (n=20) are presented in Fig. 3(f). The particle sizes varied from 55 to 512 nm depending on the experimental parameters. Between these samples, conditions A and B resulted in significantly reduced particle size ($P < 0.05$) revealing the effective role of precursor concentration ($\text{CuCl}_2 \cdot 2\text{H}_2\text{O}$) on the particle size.

Based on our results, increasing the aging time from 0 to 72 hr resulted in changing the morphology of CuO-NPs from platelets with sharp edge to spherical and rod forms. Similar result was reported by Zhou et al. [33] who worked on other kinds of precursors ($\text{Cu}(\text{NO}_3)_2 \cdot 3\text{H}_2\text{O}$ and $\text{Cu}(\text{CH}_3\text{COO})_2 \cdot \text{H}_2\text{O}$). It might be due to the reduction of surface energy in order to be thermodynamically stabilized. Longer aging time could provide enough time to reduce the surface energy of system via changing the morphology of particles from platelets to spherical type. Furthermore, the morphology of CuO-NPs can be altered via changing the type of precursor (Fig. 3(a) vs. (e)). Similar result was reported, recently [33]. Like as the crystallite size, $\text{Cu}^{2+}/\text{OH}^-$ concentration ratio also resulted in changing the morphology of particles from rod to spherical shape. While the morphology of CuO-NPs synthesized using 15 M NaOH (Fig. 3(c)) was rod-like with length of 514 ± 180 nm and thickness of 190 ± 80 nm, less NaOH concentration (1 M, Fig. 3(d)) resulted in the formation of spherical morphology with diameter of 148 ± 28 nm. This result was reported similarly for copper particles synthesized using copper (II) dodecyl sulfate ($\text{Cu}(\text{DS})_2$) precursor [34]. Increasing the concentration of $\text{Cu}(\text{DS})_2$ resulted changing the particle morphology from elongated to spherical form [34]. Since OH^- concentration strongly related to the reactions, which led to the growth of CuO nanostructures (equations 2 and 3), NaOH concentration revealed crucial role in the formation of CuO nanoparticle. The primary product of NaOH incorporation was $\text{Cu}(\text{OH})_2$ clusters which acted as nuclei for the growth of CuO nanoparticle. Based on our results, when the concentrations of Cu^{2+} and OH^- reached the critical value, CuO nuclei formed spontaneously in the aqueous solution via decomposition of $\text{Cu}(\text{OH})_2$. As the molecules at the surface of particles are vigorously less stable than the ones in the interior, in order to reduce the interfacial free energy, CuO nuclei combined together.

Therefore, it could be concluded that, the kinetic factors in aqueous solution growth of CuO could be determined by thermodynamic factors as well as the concentration of OH^- and Cu precursor.

Antibacterial activity of CuO-NPs

CuO-NPs synthesized through various conditions were also investigated with respect to the potential antibacterial applications. The antibacterial activities of the CuO-NPs were assessed against the growth of two Gram negative and positive bacteria. To determine the antibacterial activity of prepared samples against bacteria, Well-Diffusion assay was used. In this assay, the antimicrobial effects of compounds were determined by measuring the diameter in which microbial growth was inhibited (inhibition zone) reflecting the magnitude of sensitivity of the microorganism [35]. Higher extent of inhibition zone represented more active antimicrobial compound. The results of Well-Diffusion tests are shown in Table 2 (as in Table 2) and Fig. 4. All samples showed the effective bacterial inhibitory behavior. However, the magnitude of inhibitory effect on the growth of both tested bacteria was significantly related to the shapes and sizes of the particles. In this study, while samples C and E revealed the highest inhibitory effects on *St. aureus* and *E. coli*, sample D showed at least ones. Based on our results, rod-like and plate-like particles (samples C and E) resulted in the highest efficacy in inhibiting the growth of bacteria. Previously reports also demonstrated the morphology-dependent antibacterial activity in other particles [36, 37]. For instance, Wang et al. [36] showed the effects of morphology on the antibacterial characteristics of Ag_2O . Based on these studies and our results, the morphology-dependent catalytic influences can be due to higher surface active sites and surface energy of various structural morphologies [36, 38].

The antibacterial effect of CuO-NPs depended on not only their morphology and size, but also the type of microorganism. While *St. aureus* was more resistant to CuO-NPs, *E. coli* was more susceptible to them (Fig. 4 and as in Table 2). Our results were in agreement with the result of Sonia et al. [32] confirming CuO-NPs effect is more noticeable against Gram-negative bacterial strains than Gram-positive bacterial strains. The difference in the activity against these two types of bacteria could be attributed to the structural and compositional differences of the cell membrane. Gram-positive

bacteria have thicker peptidoglycan membranes compared to the Gram-negative bacteria [39]. So it was unbreakable for CuO-NPs to penetrate it and led to a low antibacterial effect [32].

Various mechanisms have been recommended to explain the antibacterial activity of

nanomaterials, such as the production of physical damage [40] and release of metal ions [26]. Physical damage is an efficient mechanism in the inhibition of bacterial growth recommended by Akhavan and Ghaderi [41]. Based on this mechanism, the bacterial cell membrane was

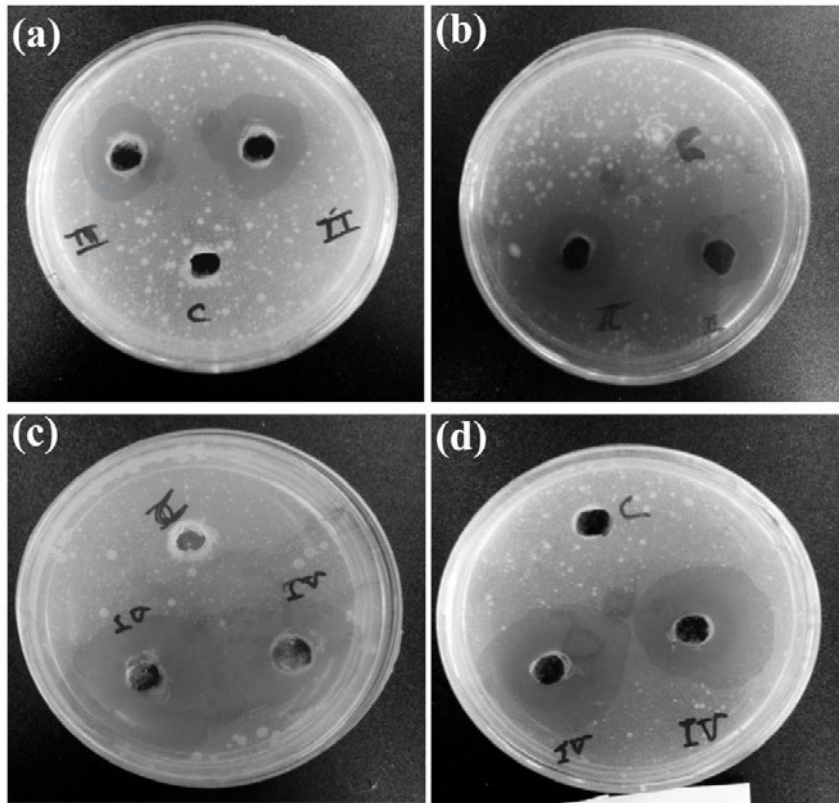


Fig. 4. Zone of inhibition of CuO nanoparticles by well-diffusion method (10 µg/well): (a) sample B against *E. coli*, (b) sample B against *S. aureus*, (c) Sample C against *E. coli*, (d) sample C against *S. aureus*. (C sign: water as control)

Table 2. The inhibition zone (mm) of CuO-NPs against pathogenic bacteria by well-diffusion method (10 µg/well) (Each data was the average of 3 replicates).

Bacteria Sample	<i>E. coli</i>	<i>St. aureus</i>
A	16.3±1.2 ^c	15.8±0.4 ^c
B	10.5±2.0 ^{de}	9.8±2.1 ^e
C	20.0±0.6 ^a	17±1.4 ^{bc}
D	10.0±0.4 ^e	12.5±0.4 ^d
E	19.3±0.7 ^{ab}	19.0±1.1 ^{ab}

Common letters above each column show insignificant difference (P>0.05).

damaged by interrelating with the sharp edges of the nanomaterials [36, 37]. Perelshtein et al. [42] demonstrated that the antibacterial activity of nano-silica silver nanocomposite could be related to this mechanism. Release of soluble ions from nanostructured metal oxide has also been suggested as an important inhibitory bacterial growth mechanism [43]. The induction of ROS after exposure to nano-metal oxides has also been demonstrated in numerous studies, leading to DNA damage and subsequently cell death [40, 42, 44]. Previous reports demonstrated the simultaneously contribution of Cu^{2+} ion release and ROS generation in the antimicrobial activity of CuO-NPs [32, 45]. Therefore, various interface characteristics have diverse chemical-physical adsorption-desorption abilities, which resulted in different antibacterial activities [32]. Based on this theory, higher surface area of the interface between bacteria and nanoparticles could be more efficient in the production of toxic copper ions resulted in superior antibacterial activity of the rod-shape particles [27]. In contrary to rod-shape and platelet-like morphologies, spherical particles provided less exposed facets resulting less inhibitory effects on the antibacterial activity. Our results are in agreement with results of Azam et al. [31] who worked on the antibacterial activity of CuO synthesized by using a gel combustion method by cupric nitrate trihydrate and citric acid and reported that the antibacterial activity of CuO-NPs is size-dependent.

CONCLUSION

In this work, we presented an eco-friendly method for synthesis CuO-NPs with various morphologies and particle sizes by using Aloe Vera leaf extract with minimum energy consuming and cost. Furthermore, the antibacterial activity of CuO-NPs against *E. coli* and *St. aureus* was investigated. Based on our results, CuO-NPs with rod, spherical and platelet-like shapes and different sizes were synthesized via changing the copper precursor type and concentration as well as aging time. Results demonstrated the formation of pure CuO-NPs with average crystallite size of 9-23 nm, depending on the functional parameters. Additionally, results demonstrated the microbial sensitivity to the CuO-NPs depended on the microbial species and also nanoparticle properties. Based on our data, CuO-NPs with rod and platelet shape morphology with bigger surface area were

more effective bacterial retardant behavior.

ACKNOWLEDGMENTS

The authors are grateful for support of this research by Isfahan University of Technology.

CONFLICT OF INTEREST

The authors declare that there are no conflicts of interest regarding the publication of this manuscript.

REFERENCES

1. Pandiyarajan T, Udayabhaskar R, Vignesh S, James RA, Karthikeyan B. Synthesis and concentration dependent antibacterial activities of CuO nanoflakes. *Mater. Sci. Eng. C Mater. Biol. Appl.*, 2013; 33(4): 2020-2024.
2. Patel VK, Bhattacharya S. High-performance nanothermite composites based on aloe-vera-directed CuO nanorods. *ACS applied materials & interfaces.*, 2013; 5(24):13364-13374.
3. Awwad AM, Albiss BA, Salem NM. Antibacterial activity of synthesized copper oxide nanoparticles using Malva sylvestris leaf extract. *SMU Med J.*, 2015; 2: 91-100.
4. He Y. A novel solid-stabilized emulsion approach to CuO nanostructured microspheres. *Mater. Res. Bull.*, 2007; 42(1):190-195.
5. Borkow G, Gabbay J. Putting copper into action: copper-impregnated products with potent biocidal activities. *The FASEB journal.*, 2004; 18(14):1728-1730.
6. Rubilar O, Rai M, Tortella G, Diez MC, Seabra AB, Durán N. Biogenic nanoparticles: copper, copper oxides, copper sulphides, complex copper nanostructures and their applications. *Biotechnol. Lett.*, 2013; 35(9):1365-1375.
7. Volanti DP, Keyson D, Cavalcante LS, Simões AZ, Joya MR, Longo E, Varela JA, Pizani PS, Souza AG. Synthesis and characterization of CuO flower-nanostructure processing by a domestic hydrothermal microwave. *J. Alloy Compd.*, 2008; 459(1): 537-542.
8. Avgouropoulos G, Ioannides T. Selective CO oxidation over CuO-CeO₂ catalysts prepared via the urea-nitrate combustion method. *Appl. Catal. A-Gen.*, 2003; 244(1): 155-167.
9. Siddique K, Nath BK, Karmakar S. Study of structural and dielectric properties of copper oxide nanoparticles prepared by wet chemical precipitation method. *Int. J. Nanosci.*, 2013; 12(05): 1350036.
10. Rodriguez-Sanchez L, Blanco MC, Lopez-Quintela MA. Electrochemical synthesis of silver nanoparticles. *J. Phys. Chem. B*, 2000; 104(41): 9683-9688.
11. Xia J, Li H, Luo Z, Shi H, Wang K, Shu H, Yan Y. Microwave-assisted synthesis of flower-like and leaf-like CuO nanostructures via room-temperature ionic liquids. *J. Phys. Chem. Solids*, 2009; 70(11): 1461-1464.
12. Zhu HT, Lin YS, Yin YS. A novel one-step chemical method for preparation of copper nanofluids. *J. Colloid. Interface. Sci.*, 2004; 277(1): 100-103.
13. Meshkani F, Rezaei M, Jafarbegloo M. Preparation of nanocrystalline Fe₂O₃-Cr₂O₃-CuO powder by a modified urea hydrolysis method: A highly active and stable catalyst for high temperature water gas shift reaction. *Mater. Res. Bull.*, 2015; 64: 418-424.

14. Lemine OM, Omri K, Zhang B, El Mir L, Sajjeddine M, Alyamani A, Bououdina M. Sol-gel synthesis of 8 nm magnetite (Fe₃O₄) nanoparticles and their magnetic properties. *Superlatt. Microstruct.*, 2012; 52(4): 793-799.
15. Eastoe J, Hollamby MJ, Hudson L. Recent advances in nanoparticle synthesis with reversed micelles. *Adv. Colloid. Interface. Sci.*, 2006; 128: 5-15.
16. Wongpisutpaisan N, Charoonsuk P, Vittayakorn N, Pecharapa W. Sonochemical synthesis and characterization of copper oxide nanoparticles. *Energy Procedia*, 2011; 9: 404-409.
17. Mittal AK, Chisti Y, Banerjee UC. Synthesis of metallic nanoparticles using plant extracts. *Biotechnol. Adv.*, 2013; 31(2): 346-356.
18. Kargar M, Reza M, Shafiee M, Ghashang M. Green Protocol Preparation of ZnO Nanoparticles in Prunus Cerasus Juice Media. *Nanosci. Nanotechnol.-Asia*, 2015; 5(1): 44-49.
19. Maensiri S, Laokul P, Klinkaewnarong J, Phokha S, Promarak V, Seraphin S. Indium oxide (In₂O₃) nanoparticles using Aloe vera plant extract: Synthesis and optical properties. *J. Optoelectron. Adv. Mater.*, 2008; 10: 161-165.
20. Herrera-Becerra R, Zorrilla C, Ascencio JA. Production of iron oxide nanoparticles by a biosynthesis method: an environmentally friendly route. *Phys. Chem. C*, 2007; 111(44): 16147-16153.
21. Philip D. Biosynthesis of Au, Ag and Au-Ag nanoparticles using edible mushroom extract. *Spectrochimica Acta Part A: Molecular and Biomolecular Spectroscopy*, 2009; 73(2): 374-381.
22. Hashoosh SI, Fadhil AM, Al-Ani NK. Production of Ag nanoparticles using Aloe vera extract and its antimicrobial activity. *J. of Al-Nahrain University.*, 2014; 17(2):165-172.
23. Phumying S, Labuayai S, Thomas C, Amornkitbamrung V, Swatsitang E, Maensiri S. Aloe vera plant-extracted solution hydrothermal synthesis and magnetic properties of magnetite (Fe₃O₄) nanoparticles. *Appl. Phys. A*, 2013; 111(4): 1187-1193.
24. Surjushe A, Vasani R, Saple DG. Aloe vera: A short review. *Indian J. Dermatol.*, 2008; 53(4):163.
25. Kumar PV, Shameem U, Kollu P, Kalyani RL, Pammi SV. Green synthesis of copper oxide nanoparticles using Aloe vera leaf extract and its antibacterial activity against fish bacterial pathogens. *BioNanoScience.*, 2015; 5(3):135-139.
26. Xiong L, Tong ZH, Chen JJ, Li LL, Yu HQ. Morphology-dependent antimicrobial activity of Cu/Cu₂O nanoparticles. *Ecotoxicology*. 2015; 24(10):2067-2072.
27. Pang H, Gao F, Lu Q. Morphology effect on antibacterial activity of cuprous oxide. *Chem. Comm.*, 2009(9): 1076-1078.
28. Nestic J, Rtimi S, Laub D, Roglic GM, Pulgarin C, Kiwi J. New evidence for TiO₂ uniform surfaces leading to complete bacterial reduction in the dark: critical issues. *Colloids and Surfaces B: Biointerfaces.*, 2014; 123: 593-599.
29. Theja GS, Lawrence RC, Ravi V, Nagarajan S, Anthony SP. Synthesis of Cu₂O micro/nanocrystals with tunable morphologies using coordinating ligands as structure controlling agents and antimicrobial studies. *CrystEngComm.*, 2014; 16: 9866-9872.
30. Gunawan C, Teoh WY, Marquis CP, Amal R. Cytotoxic origin of copper (II) oxide nanoparticles: comparative studies with micron-sized particles, leachate, and metal salts. *ACS Nano*, 2011; 5(9): 7214-7225.
31. Azam A, Ahmed AS, Oves M, Khan MS, Memic A. Size-dependent antimicrobial properties of CuO nanoparticles against Gram-positive and-negative bacterial strains. *Int. J. Nanomedicine.*, 2012; 7(9):3527-3535.
32. Sonia S, Jayram ND, Kumar PS, Mangalaraj D, Ponpandian N, Viswanathan C. Effect of NaOH concentration on structural, surface and antibacterial activity of CuO nanorods synthesized by direct sonochemical method. *Superlatt. Microstruct.*, 2014; 66:1-9.
33. Zhou K, Wang R, Xu B, Li Y. Synthesis, characterization and catalytic properties of CuO nanocrystals with various shapes. *Nanotechnology.*, 2006; 17(15): 3939.
34. Lisiecki I, Billoudet F, Pileni MP. Control of the shape and the size of copper metallic particles. *J. Phys. Chem.*, 1996; 100(10): 4160-4166.
35. Perez C, Pauli M, Bazerque P. An antibiotic assay by the agar well diffusion method. *Acta Biol. Med. Exp.*, 1990; 15(1): 113-115.
36. Wang X, Wu HF, Kuang Q, Huang RB, Xie ZX, Zheng LS. Shape-dependent antibacterial activities of Ag₂O polyhedral particles. *Langmuir*, 2009; 26(4): 2774-2778.
37. Talebian N, Amininezhad SM, Doudi M. Controllable synthesis of ZnO nanoparticles and their morphology-dependent antibacterial and optical properties. *J. Photochem. Photobiol. B: Biology.*, 2013; 120:66-73.
38. Gao P, Liu D. Facile synthesis of copper oxide nanostructures and their application in non-enzymatic hydrogen peroxide sensing. *Sensors Act. B: Chem.*, 2015; 208:346-354.
39. Madigan MT, Martinko JM, Parker J. Brock biology of microorganisms. Upper Saddle River, NJ: prentice hall; 1997.
40. Choi O, Hu Z. Size dependent and reactive oxygen species related nanosilver toxicity to nitrifying bacteria. *Environ. Sci. Technol.*, 2008; 42(12): 4583-4588.
41. Akhavan O, Ghaderi E. Toxicity of graphene and graphene oxide nanowalls against bacteria. *ACS Nano*, 2010; 4(10):5731-5736.
42. Perelshtein I, Lipovsky A, Perkas N, Gedanken A, Moschini E, Mantecca P. The influence of the crystalline nature of nano-metal oxides on their antibacterial and toxicity properties. *Nano Res.*, 2015; 8(2):695-707.
43. Misra SK, Dybowska A, Berhanu D, Luoma SN, Valsami-Jones E. The complexity of nanoparticle dissolution and its importance in nanotoxicological studies. *Sci. Total. Environ.*, 2012; 438:225-232.
44. Ruparelia JP, Chatterjee AK, Duttgupta SP, Mukherji S. Strain specificity in antimicrobial activity of silver and copper nanoparticles. *Acta Biomater.*, 2008; 4(3):707-16.
45. Ren G, Hu D, Cheng EW, Vargas-Reus MA, Reip P, Allaker RP. Characterization of copper oxide nanoparticles for antimicrobial applications. *Int. J. Antimicrob. Agents*, 2009; 33(6):587-590.